

Enhanced Fracture Resistance of Flexible ZnO:Al Thin Films in Situ Sputtered on Bent Polymer Substrates

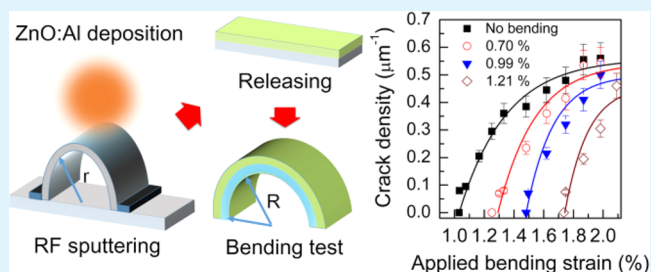
Hong Rak Choi, Senthil Kumar Eswaran, Seung Min Lee, and Yong Soo Cho*

Department of Materials Science and Engineering, Yonsei University, Seoul 120-749, Korea

Supporting Information

ABSTRACT: Improving the fracture resistance of inorganic thin films is one of the key challenges in flexible electronic devices. A nonconventional in situ sputtering method is introduced to induce residual compressive stress in ZnO:Al thin films during deposition on a bent polymer substrate. The films grown under a larger prebending strain resulted in a higher fracture resistance to applied strains by exhibiting a $\sim 70\%$ improvement in crack-initiating critical strain compared with the reference sample grown without bending. This significant improvement is attributed to the induced residual stress, which helps to prevent the formation of cracks by counteracting the applied strain.

KEYWORDS: flexible electronics, transparent conducting oxide, ZnO thin films, crack density, fracture energy



Over the past few years, fabrication of inorganic thin films on polymer substrates has been of increasing interest due to their potential applications in the field of flexible electronics.^{1–3} Nevertheless, the brittleness of inorganic thin films often results in failure of the flexible electronic devices even at low applied strains during stretching, folding and bending.^{3–6} For example, crack-initiating critical strains of inorganic thin film materials such as In₂O₃:Sn (ITO), AlN, GaAs, and Al₂O₃ were as low as 1.1, 1.4, 0.3, and 0.48%, respectively.^{1,4–7} A larger critical strain value indicates a higher crack initiation resistance in the films.

There have been a few reports suggesting strong dependences of film thickness on the fracture behavior of inorganic thin films.^{5,8–11} In particular, thin films with thickness ≥ 100 nm have exhibited poorer structural integrity on polymer substrates when subjected to various mechanical stresses.^{5,8,9} For example, recently reported fracture energy and critical strain of ZnO:Al (~ 240 nm) thin films grown on flexible polymer substrates were 68.5 J m^{-2} and 0.96%, respectively.⁵ These values were further reduced to 11.7 J m^{-2} and 0.5% for ZnO:Al thin films with a thickness of $1 \mu\text{m}$.¹⁰ The mechanical properties are a strong function of film thickness even at nanoscale thicknesses. For example, a larger critical strain of 2.4% for atomic layer-deposited Al₂O₃ thin films with a 5 nm thickness was observed compared to a critical strain of nearly 0.5% for a thickness of 80 nm.¹¹

Improving the fracture behavior of the inorganic thin films with thicknesses ≥ 100 nm is highly challenging but is required for the commercialization of flexible electronics. Residual compressive stresses developed in flexible thin films have been shown to prevent the formation of cracks, whereas tensile residual stresses facilitate crack opening and propagation.^{12–14} There have been a few reports on the effect of intentionally

induced compressive stress in inkjet-printed silver electrodes,¹⁵ e-beam evaporated metallic films¹⁶ and transferred Si ribbons¹⁷ on elastomeric poly dimethylsiloxane (PDMS) substrates using wavy, buckled surfaces to generate precompressive stress. Recently, our group demonstrated a nearly 2-fold improvement in crack-initiating critical strain (1.83%) and a $\sim 300\%$ enhancement in fracture energy (244 J m^{-2}) in the case of ZnO:Al thin films in situ deposited on a linearly stretched polymer substrate.¹⁸

In this work, improved fracture behavior of ZnO:Al films is demonstrated by another in situ sputter deposition, which uses a bent polymer substrate. The prebending of the substrate allows us to intentionally introduce residual compressive stress in the film upon release from a bending position. Despite the fact that a few efforts have been recently made to deposit inorganic ZnO, TiO₂ and ITO thin films on curved polymer substrates by one research group,^{19,20} there have been no correlative fracture studies of these films. We show that the crack-initiating critical strain and fracture energy are significantly improved to 1.74% and 299 J m^{-2} , respectively, which are significantly larger than values from earlier reports. Several quantitative values including saturated crack density, fracture energy and film strength are demonstrated to elucidate the effect of the bent surface on the improved fracture behavior as a function of curvature (or prebending strain).

Al-doped ZnO thin films were in situ sputter deposited on bent poly(ether sulfone) (PES) substrates at room temperature. A 2-in. disk-type target (99.995% purity, CERAC Inc., Milwaukee, WI) of 2 wt % Al₂O₃-doped ZnO was used for the

Received: May 30, 2015

Accepted: July 29, 2015

Published: July 29, 2015

deposition. Films of ~ 200 nm thickness were deposited at an RF power of 100 W in pure Ar atmosphere (2 mTorr). Details related to the thin film growth conditions using RF magnetron sputtering can be found in our earlier reports.^{5,6,21} Prior to the film deposition, the PES substrate was subjected to bending with a radius of curvature, r , as schematically shown in Figure 1a. Prebending of the substrate introduces a tensile strain on

ZnO:Al deposition

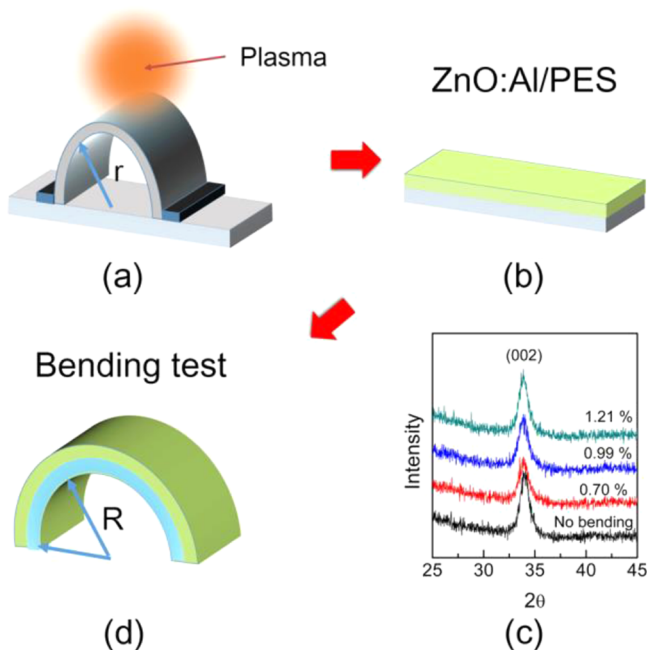


Figure 1. Schematics showing (a) the in situ sputter deposition of ZnO:Al thin film on bent PES substrate with a curvature r and (b) a ZnO:Al/PES sample released from bending after the deposition, (c) XRD patterns of the reference sample and the ZnO:Al films grown with different prebending strains, and (d) a schematic of the fracture evaluation by applying a bending radius R for the in situ processed sample.

the outside surface of the substrate. The level of tensile strain was changed by adjusting the bending radius of the PES substrate. The pretensile strain, ϵ_p , applied to the substrate was calculated using the relationship between the film/substrate thicknesses and the bending radius as given by^{5,6,8}

$$\epsilon_p = \frac{(t_f + t_s)}{2r} \frac{(1 + 2\eta + \chi\eta^2)}{(1 + \eta)(1 + \chi\eta)} \quad (1)$$

Here, t_f and t_s are the thickness of the film and substrate, respectively, $\eta = t_f/t_s$ and $\chi = E_f/E_s$. E_f and E_s are the Young's moduli (150 and 2.6 GPa) of the ZnO and PES substrate, respectively.⁶ When calculating the actual ϵ_p using eq 1, we assumed that the film thickness was zero because the pretensile stress was applied to the substrate. This simplifies eq 1 to $\epsilon_p = t_s/2r$. As a result, prebending with radius of curvature of 14.3 mm, 10.1 mm and 8.2 mm creates tensile strains of 0.70, 0.99, and 1.21%, respectively. We identify these tensile strains caused by bending of the substrate, as "prebending strain" for the remainder of this paper. The PES substrate in the bent position was transferred to the sputtering chamber. ZnO:Al films were deposited on the bent PES substrates with different bending radii. After film growth, the ZnO:Al/PES structure was released from its bent position to a normal position (Figure 1b).

The structure of the released films was analyzed using an X-ray diffractometer (XRD: Max-2500, Rigaku B) under Cu-K α radiation, as shown in Figure 1c. The XRD patterns reveal that the ZnO:Al films are highly oriented along the (002) direction of wurtzite hexagonal structure. The peak position of the (002) reflection shifted toward smaller 2θ values with increasing prebending strain. This suggests that the prebending strain induces residual compressive stresses in the deposited films. By using a known biaxial strain model,²² the residual stresses relative to the unbent reference sample were estimated as -2.08 , -2.34 , and -2.84 N m $^{-2}$ for films deposited with prebending strain of 0.70, 0.99, and 1.21%, respectively.

The fracture behavior concerning the formation of cracks in the deposited/released films was monitored as the samples were subjected to an applied bending strain, ϵ_a , as shown in Figure 1d. The applied bending strain was calculated by measuring the radius of curvature R of the film structure using the identical eq 1 as described elsewhere.^{5,6,10} For example, the ϵ_a value was estimated to be in the range of 0.99–2.09% for a bending radius (R) range of 10.07 to 4.77 mm. Actual cracks on the ZnO:Al films after applying the bending strain were observed using an optical microscope (LV150 BD DIC, Nikon, Japan) to quantify the evolution of cracks with different bending levels.

Crack formation against the applied bending strain, ϵ_a , can be described in terms of crack density, ρ , which is defined as the number of parallel cracks per unit micrometer length. Figure 2a

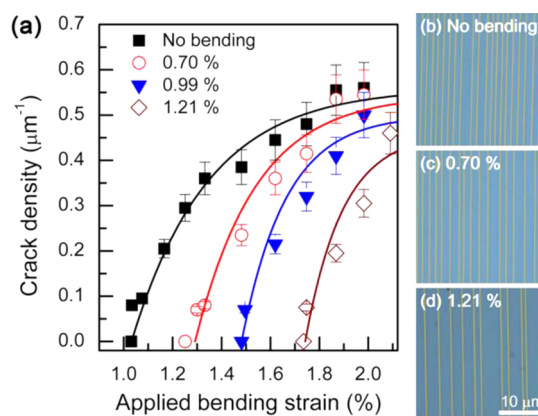


Figure 2. (a) Dependence of the crack density on the applied bending strain of the reference sample and the ZnO:Al films grown with prebending strain of 0.70, 0.99, and 1.21%. The solid lines represent the least-squares fits to data points. The selected optical micrographs correspond to (b) the reference sample and the ZnO:Al films grown with prebending strains of (c) 0.70% and (d) 1.21% after the bending trials at an applied bending strain of 1.98%. The same scale bar for all the images is given in d.

shows the variations in crack density as a function of applied bending strain for ZnO:Al films grown with prebending strains of 0.70, 0.99, and 1.21%. For comparison, a reference sample grown without bending of the substrate is included. A similar trend was observed for all the samples regardless of the prebending strain. All the films withstood the applied bending strain up to a threshold value, called critical strain, ϵ_c , below which no cracks were observed. When the applied bending strain increased beyond a critical strain ($\epsilon_a > \epsilon_c$), the formation of cracks perpendicular to the bending direction began and the crack density rapidly increased with a further increase in the applied bending strain.

Figure 2b–d show selected examples of optical micrograph images depicting parallel cracks on the surface of ZnO:Al films at identical ϵ_a values of 1.98%; at this strain, the crack density was nearly saturated. The micrographs were photoedited with blue background for better contrast visualization. The cracks were well isolated, parallel and extended to the entire surface of the sample. The micrographs clearly reveal that the number of cracks for a given area decreased with increasing prebending strain ϵ_p . As a result, the crack spacing λ , which is defined as the distance between two adjacent cracks, increased. Generally, the crack spacing and the crack density have an inverse relationship, as the crack spacing approaches infinity when no cracks are observed. We estimated the average crack spacing at the saturated stage using the simple relation $\lambda = 1/\rho_s$. The crack spacing varied from 1.8 μm for the reference sample to 2.4 μm for the sample grown with the highest ϵ_p value of 1.21%.

The change in crack density with applied bending strain in Figure 2a was further examined by fitting the values using an equation of exponential form¹¹

$$\rho = \rho_s \{1 - \exp[-b(\epsilon_a - \epsilon_c)]\} \quad (2)$$

where ρ_s is the saturated crack density and b is the fitting parameter. The solid lines in Figure 2a represent the fitting curves. Crack-initiating critical strain (ϵ_c) values were 1.03, 1.29, 1.48, and 1.74% corresponding to the reference sample and the samples with prebending strains of 0.70, 0.99, and 1.21%, respectively. These results show that the critical strain shifts toward a higher value with increasing prebending strain. The corresponding saturated crack densities, ρ_s , were 0.56 μm^{-1} (reference sample), 0.54 μm^{-1} (0.70%), 0.50 μm^{-1} (0.99%), and 0.46 μm^{-1} (1.21%).

The values of ϵ_c and ρ_s obtained for increasing ϵ_p are shown in Figure 3a, b. Horizontal dotted lines represent the values that

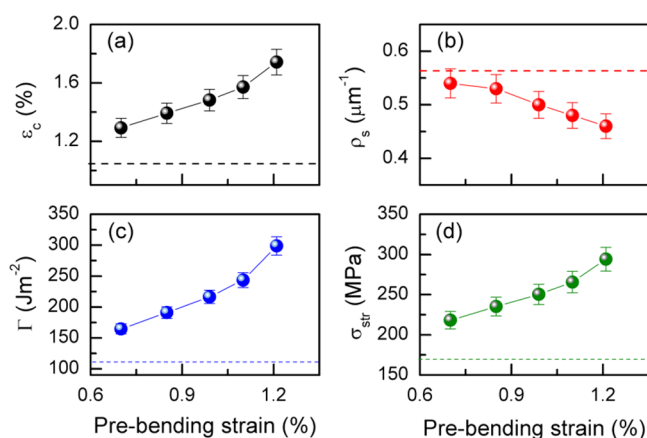


Figure 3. Dependence of the (a) critical strain, (b) saturated crack density, (c) fracture energy, and (d) film strength on the prebending strain of the PES substrate. The horizontal dotted lines represent corresponding values for the reference sample.

correspond to the reference sample. The highest ϵ_c value of 1.74% is a nearly 70% improvement when compared with the reference sample. Previously reported critical strains for ZnO thin films are in the range of 0.5–1.1%.^{5,6,10} ZnO:Al thin films passivated with an AlN layer exhibited critical strain of 1.9%.⁶ Hence, the observed critical strain of 1.74% is meaningful when considered a higher thickness of ~ 200 nm without a passivation layer. In addition, the saturated crack density showed a monotonic decrease with increasing prebending strain. This

clearly demonstrates that prebending strain during film growth had a positive effect on the cracking behavior. The improved fracture resistance can be understood from the viewpoint of interatomic spacing and bond energy of ZnO:Al thin films.^{12,23,24} The residual compressive stress in ZnO:Al films may reduce the interatomic spacing and hence the bond length relative to those of the reference ZnO. Reduction in bond length may result in the increases of bond strength and bond dissociation energy of ZnO. In general, the bond length is inversely related to the bond strength.^{23,24} Therefore, a larger energy is required to break the bonds for crack initiation. Conclusively, the residual compressive stress builds an additional energy barrier for the ZnO:Al film cracking, which increases with the level of applied bending stress.

To further investigate the effect of prebending strain on the fracture behavior of the ZnO:Al films, we estimated the fracture energy, Γ , and the film strength, σ_{str} using the energy and strength criterion, respectively, proposed earlier for multiple cracking of thin films on polymer substrates.^{25–28} The detailed procedure used for obtaining Γ and σ_{str} values is described in the Supporting Information. Figure 3c, d show the plots of fracture energy and film strength with different prebending strain. As expected, both the fracture energy and film strength monotonically increase with increasing prebending strain, indicating the positive effect of the residual compressive stress. The ZnO:Al film grown with a prebending strain of 1.21% exhibited the highest fracture energy of ~ 299 J m^{-2} and a film strength of ~ 294 MPa, which can be compared to the corresponding values of ~ 105 J m^{-2} and 174 MPa for the reference sample.

In the literature, flexible ZnO films grown on various polymer substrates have showed fracture energies in the range of 49 to 142 J m^{-2} .^{6,10} Hence, the observed fracture energy of 299 J m^{-2} here is a significant enhancement, indicating that a much higher physical energy is required to initiate cracks in the films having extra compressive stress. These results also suggest that the current in situ method may be competitive in creating very crack-resistance films by adopting a simple curved flexible substrate design. In addition, mode I fracture toughness, K_{IC} , was obtained by using the simple relation $\Gamma = K_{IC}^2/E_f$.⁵ These values were 3.9 $\text{MPa m}^{1/2}$ and 6.7 $\text{MPa m}^{1/2}$ for the reference and the $\epsilon_p \approx 1.21\%$ films, respectively. Earlier reported values of K_{IC} for ZnO, ITO and Al_2O_3 films were in the range of 2–4 $\text{MPa m}^{1/2}$.^{6,10,11} All mechanical parameters obtained using the proposed in situ method support the positive effects of extra compressive stress on fracture behavior of the ZnO:Al films.

In conclusion, ZnO:Al thin films were successfully in situ sputter-deposited on bent polymer substrates. This method introduces residual compressive stress intentionally in the films, which is controllable with the level of prebending curvature. The effect of extra compressive stress on the fracture behavior of the films was evaluated by bending the deposited films with various bending levels, and by counting the number of cracks developed on the films. As a significant indicator, the crack-initiating critical strain was substantially improved from 1.03 to 1.74% with increasing the residual compressive strain in the films. All other mechanical parameters, such as saturated crack density, fracture energy, films strength and fracture toughness, indicate that the proposed in situ method is an effective way of inducing a much higher mechanical failure resistance against flexible environments.

■ ASSOCIATED CONTENT

Supporting Information

The Supporting Information is available free of charge on the ACS Publications website at DOI: 10.1021/acsami.5b04727.

Detailed procedures related to the calculation of fracture energy and film strength in the ZnO/PES structures (PDF)

■ AUTHOR INFORMATION

Corresponding Author

*E-mail: ycho@yonsei.ac.kr. Tel: 82-2-2123-5848.

Notes

The authors declare no competing financial interest.

■ ACKNOWLEDGMENTS

This work was financially supported by grants (2011-0020285 and 2013R1A2A2A01016711) from the National Research Foundation of Korea (NRF) funded by the Korean government.

■ REFERENCES

- (1) Park, K.; Lee, D. K.; Kim, B. S.; Jeon, H.; Lee, N. E.; Whang, D.; Lee, H. J.; Kim, Y. J.; Ahn, J. H. Stretchable, Transparent Zinc Oxide Thin Film Transistors. *Adv. Funct. Mater.* **2010**, *20*, 3577–3582.
- (2) Wang, W.; Han, D.; Cai, J.; Geng, Y.; Wang, L.; Wang, L.; Tian, Y.; Zhang, X.; Wang, Y.; Zhang, S. Fully Transparent Al-Doped ZnO Thin-Film Transistors on Flexible Plastic Substrates. *Jpn. J. Appl. Phys.* **2013**, *52*, 04CF10.
- (3) Gutruf, P.; Shah, C. M.; Walia, S.; Nili, H.; Zoolfaker, A. S.; Karnutsch, C.; Kalantar-zadeh, K.; Sriram, S.; Bhaskaran, M. Transparent Functional Oxide Stretchable Electronics: Micro-Tectonics Enabled High Strain Electrodes. *NPG Asia Mater.* **2013**, *5*, e62.
- (4) Chae, S. H.; Yu, W. J.; Bae, J. J.; Duong, D. L.; Perello, D.; Jeong, H. Y.; Ta, Q. H.; Ly, T. H.; Vu, Q. A.; Yun, M.; Duan, X.; Lee, Y. H. Transferred Wrinkled Al₂O₃ for Highly Stretchable and Transparent Graphene–Carbon Nanotube Transistors. *Nat. Mater.* **2013**, *12*, 403–409.
- (5) Mohanty, B. C.; Choi, H. R.; Choi, Y. M.; Cho, Y. S. Thickness-Dependent Fracture Behaviour of Flexible ZnO:Al Thin Films. *J. Phys. D: Appl. Phys.* **2011**, *44*, 025401.
- (6) Choi, H. R.; Mohanty, B. C.; Kim, J. S.; Cho, Y. S. AlN Passivation Layer-Mediated Improvement in Tensile Failure of Flexible ZnO:Al Thin Films. *ACS Appl. Mater. Interfaces* **2010**, *2*, 2471–2474.
- (7) Chen, Z.; Cotterell, B.; Wang, W.; Guenther, E.; Chua, S. J. A Mechanical Assessment of Flexible Optoelectronic Devices. *Thin Solid Films* **2001**, *394*, 202–205.
- (8) Park, S. I.; Ahn, J. H.; Feng, X.; Wang, S.; Huang, Y.; Rogers, J. A. Theoretical and Experimental Studies of Bending of Inorganic Electronic Materials on Plastic Substrates. *Adv. Funct. Mater.* **2008**, *18*, 2673–2684.
- (9) Heinrich, M.; Gruber, P.; Orso, S.; Handge, U. A.; Spolenak, R. Dimensional Control of Brittle Nanoplatelets. A Statistical Analysis of a Thin Film Cracking Approach. *Nano Lett.* **2006**, *6*, 2026–2030.
- (10) Ni, J. L.; Zhu, X. F.; Pei, Z. L.; Gong, J.; Sun, C.; Zhang, G. P. Comparative Investigation of Fracture Behaviour of Aluminium-Doped ZnO Films on a Flexible Substrate. *J. Phys. D: Appl. Phys.* **2009**, *42*, 175404.
- (11) Jen, S. H.; Bertrand, J. A.; Geroge, S. M. Critical Tensile and Compressive Strains for Cracking of Al₂O₃ Films Grown by Atomic Layer Deposition. *J. Appl. Phys.* **2011**, *109*, 084305.
- (12) Huang, Y. C.; Chang, S. Y.; Chang, C. H. Effect of Residual Stresses on Mechanical Properties and Interface Adhesion Strength of SiN Thin Films. *Thin Solid Films* **2009**, *517*, 4857–4861.

(13) Xia, Z.; Curtin, W. A.; Sheldon, B. W. A New Method to Evaluate the Fracture Toughness of Thin Films. *Acta Mater.* **2004**, *52*, 3507–3517.

(14) Bhowmick, S.; Kale, A. N.; Jayaram, V.; Biswas, S. K. Contact Damage in TiN Coatings on Steel. *Thin Solid Films* **2003**, *436*, 250–258.

(15) Lee, J.; Chung, S.; Song, H.; Kim, S.; Hong, Y. Lateral-Crack-Free, Buckled, Inkjet-Printed Silver Electrodes on Highly Pre-Stretched Elastomeric Substrates. *J. Phys. D: Appl. Phys.* **2013**, *46*, 105305.

(16) Bowden, N.; Brittain, S.; Evans, A. G.; Hutchinson, J. W.; Whitesides, G. M. Spontaneous Formation of Ordered Structures in Thin Films of Metals Supported on an Elastomeric Polymer. *Nature* **1998**, *393*, 146–149.

(17) Khang, D. Y.; Jiang, H.; Huang, Y.; Rogers, J. A. A Stretchable Form of Single-Crystal Silicon for High-Performance Electronics on Rubber Substrates. *Science* **2006**, *311*, 208–212.

(18) Choi, H. R.; Eswaran, S. K.; Cho, Y. S. Prestress Driven Improvement in Fracture Behavior of In Situ Sputtered Zinc Oxide Thin Films on Stretched Polymer Substrates. *ACS Appl. Mater. Interfaces* **2015**, *7*, 14654.

(19) Hsieh, P. T.; Li, T. C.; Wu, B. H.; Chung, C. J.; Lin, J. F. Structural and Mechanical Properties of Pre-Strained Transparent Conducting Oxide Films on Flexible Substrate. *Surf. Coat. Technol.* **2013**, *231*, 443–446.

(20) Li, T. C.; Wu, B. H.; Lin, J. F. Effects of Pre-Strain Applied at a Polyethylene Terephthalate Substrate Before the Coating of TiO₂ Film on the Coating Film Quality and Optical Performance. *Thin Solid Films* **2011**, *519*, 7875–7882.

(21) Mohanty, B. C.; Jo, Y. H.; Yeon, D. H.; Choi, I. J.; Cho, Y. S. Stress-Induced Anomalous Shift of Optical Band Gap in ZnO:Al Thin Films. *Appl. Phys. Lett.* **2009**, *95*, 062103.

(22) Maniv, S.; Westwood, W. D.; Colombini, E. Pressure and Angle of Incidence Effects in Reactive Planar Magnetron Sputtered ZnO Layers. *J. Vac. Sci. Technol.* **1982**, *20*, 162–170.

(23) Zhang, X.; Watanabe, N.; Kuroda, S. Effects of Residual Stress on the Mechanical Properties of Plasma-Sprayed Thermal Barrier Coatings. *Eng. Fract. Mech.* **2013**, *110*, 314–327.

(24) Kang, I. J.; Woo, S. A.; Park, C. H. First-Principles Study of the Atomic and Electronic Structure of Amorphous ZnO-SiO₂. *J. Korean Phys. Soc.* **2011**, *58*, 604–607.

(25) Zhang, X. C.; Liu, C. J.; Xuan, F. Z.; Wang, Z. D.; Tu, S. T. Effect of Residual Stresses on the Strength and Fracture Energy of the Brittle Film: Multiple Cracking Analysis. *Comput. Mater. Sci.* **2010**, *50*, 246–252.

(26) Hsueh, C. H.; Yanaka, M. Multiple Film Cracking in Film/Substrate Systems with Residual Stresses and Unidirectional Loading. *J. Mater. Sci.* **2003**, *38*, 1809–1817.

(27) Hsueh, C. H.; Wereszczak, A. A. Multiple Cracking of Brittle Coatings on Strained Substrates. *J. Appl. Phys.* **2004**, *96*, 3501–3506.

(28) Gao, Y.; Wang, Z. L. Equilibrium Potential of Free Charge Carriers in a Bent Piezoelectric Semiconductive Nanowire. *Nano Lett.* **2009**, *9*, 1103–1110.